Characterizing ultrabroadband attosecond lasers

Michael Chini,[1] Steve Gilbertson,[1] Sabih D. Khan,[1] and Zenghu Chang[1,2,*]

[1]*J. R. Macdonald Laboratory, Department of Physics, Kansas State University, Manhattan 66502, Kansas, USA*
[2]*CREOL and Department of Physics, University of Central Florida, Orlando 32816, Florida, USA*
**chang@phys.ksu.edu*

Abstract: Recent progress in sub-laser-cycle gating of high-order harmonic generation promises to push the limits on optical pulse durations below the atomic unit of time, 24 *as*, which corresponds to a bandwidth broader than 75 eV. However, the available techniques for attosecond pulse measurement are valid only for narrow-bandwidth spectra, due to one of the key approximations made in the phase retrieval. Here we report a new technique for characterizing attosecond pulses, whereby the spectral phase of the attosecond pulse is extracted from the oscillation component with the dressing laser frequency in the photoelectron spectrogram. This technique, termed PROOF (Phase Retrieval by Omega Oscillation Filtering), can be applied to characterizing attosecond pulses with ultrabroad bandwidths.

©2010 Optical Society of America

OCIS codes: (320.7100) Ultrafast measurements; (140.7240) UV, EUV, and X-ray lasers.

References and links

1. E. Goulielmakis, M. Schultze, M. Hofstetter, V. S. Yakovlev, J. Gagnon, M. Uiberacker, A. L. Aquila, E. M. Gullikson, D. T. Attwood, R. Kienberger, F. Krausz, and U. Kleineberg, "Single-cycle nonlinear optics," Science **320**(5883), 1614–1617 (2008).
2. H. Mashiko, S. Gilbertson, M. Chini, X. Feng, C. Yun, H. Wang, S. D. Khan, S. Chen, and Z. Chang, "Extreme ultraviolet supercontinua supporting pulse durations of less than one atomic unit of time," Opt. Lett. **34**(21), 3337–3339 (2009).
3. G. Sansone, F. Ferrari, C. Vozzi, F. Calegari, S. Stagira, and M. Nisoli, "Towards atomic unit pulse duration by polarization-controlled few-cycle pulses," J. Phys. B **42**(13), 134005 (2009).
4. F. Quéré, Y. Mairesse, and J. Itatani, "Temporal characterization of attosecond XUV fields," J. Mod. Opt. **52**(2), 339–360 (2005).
5. E. Cormier, I. A. Walmsley, E. M. Kosik, A. S. Wyatt, L. Corner, and L. F. Dimauro, "Self-referencing, spectrally, or spatially encoded spectral interferometry for the complete characterization of attosecond electromagnetic pulses," Phys. Rev. Lett. **94**(3), 033905 (2005).
6. J. Itatani, F. Quéré, G. L. Yudin, M. Yu. Ivanov, F. Krausz, and P. B. Corkum, "Attosecond streak camera," Phys. Rev. Lett. **88**(17), 173903 (2002).
7. R. Kienberger, E. Goulielmakis, M. Uiberacker, A. Baltuska, V. Yakovlev, F. Bammer, A. Scrinzi, Th. Westerwalbesloh, U. Kleineberg, U. Heinzmann, M. Drescher, and F. Krausz, "Atomic transient recorder," Nature **427**(6977), 817–821 (2004).
8. Y. Mairesse, and F. Quéré, "Frequency-resolved optical gating for complete reconstruction of attosecond bursts," Phys. Rev. A **71**(1), 011401 (2005).
9. J. Gagnon, E. Goulielmakis, and V. S. Yakovlev, "The accurate FROG characterization of attosecond pulses from streaking measurements," Appl. Phys. B **92**(1), 25–32 (2008).
10. G. Sansone, E. Benedetti, F. Calegari, C. Vozzi, L. Avaldi, R. Flammini, L. Poletto, P. Villoresi, C. Altucci, R. Velotta, S. Stagira, S. De Silvestri, and M. Nisoli, "Isolated single-cycle attosecond pulses," Science **314**(5798), 443–446 (2006).
11. X. Feng, S. Gilbertson, H. Mashiko, H. Wang, S. D. Khan, M. Chini, Y. Wu, K. Zhao, and Z. Chang, "Generation of isolated attosecond pulses with 20 to 28 femtosecond lasers," Phys. Rev. Lett. **103**(18), 183901 (2009).
12. H. Wang, M. Chini, S. D. Khan, S. Chen, S. Gilbertson, X. Feng, H. Mashiko, and Z. Chang, "Practical issues of retrieving isolated attosecond pulses," J. Phys. At. Mol. Opt. Phys. **42**(13), 134007 (2009).
13. M. Kitzler, N. Milosevic, A. Scrinzi, F. Krausz, and T. Brabec, "Quantum theory of attosecond XUV pulse measurement by laser dressed photoionization," Phys. Rev. Lett. **88**(17), 173904 (2002).
14. S. Gilbertson, Y. Wu, S. D. Khan, M. Chini, K. Zhao, X. Feng, and Z. Chang, "Isolated attosecond pulse generation using multicycle pulses directly from a laser amplifier," Phys. Rev. A **81**(4), 043810 (2010).
15. T. Baumert, T. Brixner, V. Seyfried, M. Strehle, and G. Gerber, "Femtosecond pulse shaping by an evolutionary algorithm with feedback," Appl. Phys. B **65**(6), 779–782 (1997).

#126449 - $15.00 USD Received 2 Apr 2010; revised 24 May 2010; accepted 24 May 2010; published 2 Jun 2010
(C) 2010 OSA

16. D. J. Kane, "Principal components generalized projections: a review," J. Opt. Soc. Am. B **25**(6), A120–A132 (2008).
17. P. M. Paul, E. S. Toma, P. Breger, G. Mullot, F. Augé, Ph. Balcou, H. G. Muller, and P. Agostini, "Observation of a train of attosecond pulses from high harmonic generation," Science **292**(5522), 1689–1692 (2001).

1. Introduction

Single isolated attosecond pulses are an exciting new tool for probing electron dynamics in matter. Already, isolated pulses with 80 *as* durations have been generated and fully characterized [1]. Generation of attosecond pulses with much shorter pulse durations has not been limited by the available bandwidth of the extreme ultraviolet (XUV) light, as continuum spectra supporting pulse durations of 16 *as* and 45 *as* have recently been produced using double optical gating (DOG) [2] and polarization gating (PG) [3]. However, such pulses could not be temporally characterized with current pulse measurement techniques.

Accurate characterization of the temporal profile of isolated attosecond pulses is critical for the development of new attosecond light sources and for using such pulses in pump-probe experiments. Although other methods such as XUV SPIDER have been proposed [4,5], the measurement of isolated attosecond pulses has so far been performed with the attosecond streak camera or attosecond transient recorder technique [6,7], whereby the attosecond XUV pulse is converted into its electron replica through photoemission in atoms. The electrons are then momentum-shifted in a near infrared (NIR) laser field. The electron spectrum is measured as a function of the delay between the XUV and NIR pulses, and the time information of the attosecond pulse is encoded in the streaked photoelectron spectrum using the classical time-to-momentum conversion relationship. The motion of the free electron in the NIR field can be treated classically for the strong NIR lasers used in the measurement. The streaked photoelectron spectrogram can then be used to retrieve the attosecond pulse, a technique known as FROG-CRAB (Frequency-Resolved Optical Gating for Complete Reconstruction of Attosecond Bursts) [8,9]. The attosecond pulse is retrieved by matching the measured spectrogram to a FROG-CRAB trace reconstructed from a guessed pulse amplitude and phase.

The FROG-CRAB technique has a major limitation. It assumes that the bandwidth of the attosecond pulse is much smaller than the central energy of the photoelectrons. This central momentum approximation is needed to apply the FROG phase retrieval techniques developed for measurement of femtosecond lasers [8], and it poses a limitation on the shortest attosecond pulses that can be characterized at a given center photon energy. Even in the current state-of-the-art experiments [1,10,11], the central momentum approximation is only barely met, and measurement of even shorter pulses would almost certainly violate the approximation. Furthermore, in the attosecond streaking model, the time resolution is determined by the streaking laser intensity. High NIR laser intensity is needed so that the amount of broadening of the electron spectrum width is comparable to the bandwidth of the attosecond pulse to be measured [6], which requires intensity greater than 10^{14} W/cm^2 to characterize a 70 *as* pulse centered at 100 eV [6,8]. More recent work indicates that the streaking model overestimates the required streaking intensity for FROG-CRAB [12], but that high intensities are still required to measure even shorter pulses. For characterizing 25 *as* pulses centered at 100 eV, the required laser intensity would produce high-energy photoelectrons through multiphoton and field ionization of the target atoms, which would overlap with the attosecond photoelectron spectrum and destroy much of the information encoded in the streaked spectrogram.

2. Principle of PROOF

An isolated attosecond pulse can be described by the Fourier transform

$$\varepsilon_X(t) = \int_{-\infty}^{\infty} U(\omega) e^{i\phi(\omega)} e^{i\omega t} \mathrm{d}\omega. \quad (1)$$

#126449 - $15.00 USD Received 2 Apr 2010; revised 24 May 2010; accepted 24 May 2010; published 2 Jun 2010
(C) 2010 OSA

Because it is relatively easy to measure the power spectrum $I(\omega) = |U(\omega)|^2$, only an accurate measurement of the spectral phase $\phi(\omega)$ is needed to fully describe the pulse. Here we show that the phase of isolated attosecond pulses can be accurately measured using spectral interference from laser-assisted photoemission signals, a technique we term PROOF (Phase Retrieval by Omega Oscillation Filtering). It requires only modest dressing laser intensities and is not limited by the attosecond spectrum bandwidth.

For the characterization of isolated attosecond XUV pulses with PROOF, the laser-assisted photoemission technique is used [13]. The experimental setup for obtaining the electron spectrogram is very similar to what is used for FROG-CRAB, except that the dressing laser intensity can be much lower. Once the detection atoms with ionization potential I_p absorb XUV photons with frequency ω_v, free electrons with momentum $\vec{v}$ are produced through the dipole transition from the ground state, where $\omega_v = v^2/2 + I_p$ in atomic units. At a given delay between the attosecond pulse and the NIR field, the laser field changes the spectral distribution of those electrons. The spectrum of photoelectrons produced by the XUV pulse in the presence of a NIR field is measured as a function of the time delay τ between the XUV and NIR pulses. The difference between PROOF and the streaking-based FROG-CRAB is in the mechanism of phase encoding in the electron spectrogram and the method of phase retrieval.

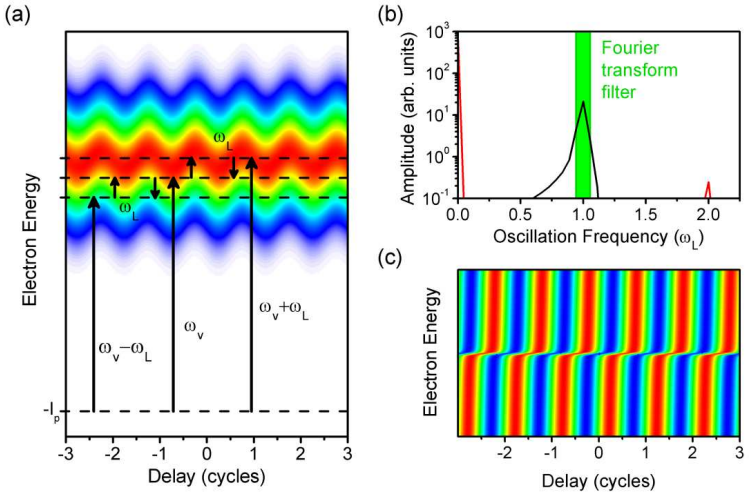

Fig. 1. Principle of PROOF. (a) The isolated attosecond pulse photoionizes electrons to continuum states. Those continuum states separated by the laser central frequency ω_L are coupled by the dressing laser, leading to the characteristic oscillation of the photoelectron signal with delay. (b) Fourier transform amplitude of the signal from one electron energy in (a). Peaks are found at oscillation frequencies of zero (red line), ω_L (black line), and $2\omega_L$ (red line). The ω_L component is selected using a filter. (c) Spectrogram obtained by inverse Fourier transform of the filtered ω_L component of the oscillation, from which the phase angle $\alpha(v)$ can be extracted.

The spectral phase encoding in PROOF can be described by quantum interference of the continuum states caused by the dressing laser. The interference of those states coupled by the dressing laser causes the electron signal at a constant energy to oscillate with the delay, as illustrated in Fig. 1(a). This sinusoidal oscillation is governed by the amplitude and phase of each of the interfering spectral components. When the component of the oscillation with the

#126449 - $15.00 USD Received 2 Apr 2010; revised 24 May 2010; accepted 24 May 2010; published 2 Jun 2010
(C) 2010 OSA

dressing laser central frequency ω_L is extracted, as shown in Fig. 1(b) and (c), the interference is related to the spectral phases $\phi(\omega_v - \omega_L)$, $\phi(\omega_v)$, and $\phi(\omega_v + \omega_L)$ of the three XUV frequency components separated by the laser photon energy. The spectral phase can therefore be decoded from the ω_L oscillation of the signal at each energy, measured as a function of delay between the XUV pulse and the NIR field.

To decode the spectral phase difference, one needs to find the spectral phase that matches the sinusoidal oscillations. Retrieving the spectral phase from these oscillations reduces to a minimization problem described below. Unlike FROG-CRAB, this method does not use FROG phase retrieval algorithms, and the central momentum approximation is not needed. Furthermore, observation of this oscillation does not require high streaking intensities, as only one NIR photon is needed to couple the continuum states. We calculate that the oscillation amplitude at a photoelectron energy of 10 eV is more than 20% of the spectrum intensity for a dressing laser intensity of 10^{11} W/cm^2. Therefore, PROOF can be used with NIR laser intensities that produce far fewer background electrons than what is needed for streaking.

2.1 Derivation

When a linearly polarized NIR laser is used to dress the photoionization from an isolated attosecond XUV pulse, the detected photoelectron spectrum is altered by the dressing laser. For simplicity, we assume that the NIR and XUV fields are polarized in the same direction and only the electrons emitted along the laser electric field direction are detected. Then, the amplitude of the electron wave function detected with momentum v with a delay τ_d between the XUV and NIR pulses is given (in atomic units) by [8]:

$$b(v,\tau_d) = -i\int_{-\infty}^{\infty} \varepsilon_X(t-\tau) d[v+A(t)] e^{i\varphi(t)} e^{-i(v^2/2+I_p)t} \mathrm{d}t, \tag{2}$$

$$\varphi(t) = -\int_t^{\infty} [vA(t') + A^2(t')/2] \mathrm{d}t', \tag{3}$$

where $\varepsilon_X(t)$ is the electric field of the attosecond pulse, $A(t)$ is the vector potential of the laser field $\varepsilon_L(t) = -\frac{\partial A}{\partial t}$, $v + A(t)$ is the instantaneous momentum of the photoionized electron in the laser field, $d[v]$ is the complex transition matrix element from the ground state to the continuum state with momentum v [8,9,13]. For convenience, we assume the transition matrix element to be constant.

For low intensity laser fields under the slowly-varying envelope approximation, $\varepsilon_L(t) = E_0(t)\cos(\omega_L t)$, as are typically used for dressing the attosecond photoionization, the phase modulation to the electron wave by the laser field is given by [8]:

$$\varphi(t) = -\int_t^{\infty} \frac{E_0^2(t)}{4\omega_L^2} \mathrm{d}t + \frac{vE_0}{2\omega_L^2}\cos(\omega_L t) - \frac{E_0^2}{8\omega_L^3}\sin(2\omega_L t), \tag{4}$$

or, approximately:

$$\varphi(t) \approx \frac{vE_0}{2\omega_L^2}\cos(\omega_L t) = \frac{vE_0}{2\omega_L^2}(e^{i\omega_L t} + e^{-i\omega_L t}). \tag{5}$$

When the energy shift of the streaking is much less than the energy of a single NIR photon (i.e., $\frac{vE_0}{2\omega_L} << \omega_L$), then

$$e^{i\varphi(t)} \approx 1 + i\varphi(t). \tag{6}$$

#126449 - $15.00 USD Received 2 Apr 2010; revised 24 May 2010; accepted 24 May 2010; published 2 Jun 2010
(C) 2010 OSA

Then, the amplitude of the electron wavepacket is given by:

$$b(v,\tau_d) \propto \int_{-\infty}^{\infty} \varepsilon_X(t-\tau)[1+i\frac{vE_0}{2\omega_L^2}(e^{i\omega_L t}+e^{-i\omega_L t})]e^{-i(v^2/2+I_p)t}\mathrm{d}t. \quad (7)$$

Then, integration of Eq. (7), substituting Eq. (1) for the XUV pulse yields:

$$\begin{aligned} b(v,\tau_d) \approx e^{-i\omega_v\tau_d}\{&U(\omega_v)e^{i\phi(\omega_v)} \\ &+i\frac{vE_0}{2\omega_L^2}[U(\omega_v+\omega_L)e^{i\phi(\omega_v+\omega_L)}e^{-i\omega_L\tau_d}+U(\omega_v-\omega_L)e^{i\phi(\omega_v-\omega_L)}e^{i\omega_L\tau_d}]\}, \end{aligned} \quad (8)$$

where $\omega_v = v^2/2 + I_p$ is the photon energy associated with the photoelectron momentum v.

The measured signal then has three components, $I(v,\tau_d) = |b(v,\tau_d)|^2 \approx I_0 + I_{\omega_L} + I_{2\omega_L}$, where $I_0(v,\tau_d) = U^2(\omega_v)$ does not change with the delay, I_{ω_L} oscillates with ω_L along the delay axis, and $I_{2\omega_L}$ oscillates with $2\omega_L$. We are only interested in the I_{ω_L} component:

$$\begin{aligned} I_{\omega_L} = i\frac{vE_0}{2\omega_L}[&-U(\omega_v)U(\omega_v+\omega_L)e^{i[\phi(\omega_v)-\phi(\omega_v+\omega_L)]}e^{i\omega_L\tau_d} \\ &+U(\omega_v)U(\omega_v+\omega_L)e^{i[\phi(\omega_v+\omega_L)-\phi(\omega_v)]}e^{-i\omega_L\tau_d}+U(\omega_v)U(\omega_v-\omega_L)e^{i[\phi(\omega_v)-\phi(\omega_v-\omega_L)]}e^{-i\omega_L\tau_d} \\ &-U(\omega_v)U(\omega_v-\omega_L)e^{i[\phi(\omega_v-\omega_L)-\phi(\omega_v)]}e^{i\omega_L\tau_d}]. \end{aligned} \quad (9)$$

The $U(\omega_v)U(\omega_v+\omega_L)e^{i[\phi(\omega_v)-\phi(\omega_v+\omega_L)]}e^{i\omega_L\tau_d}$ term can be considered as from the two-photon transition that involves one XUV photon ω_v plus one NIR photon ω_L. The final state is at $\omega_v+\omega_L$. This transition reduces the signal at ω_v. Similarly, the $U(\omega_v)U(\omega_v+\omega_L)e^{i[\phi(\omega_v+\omega_L)-\phi(\omega_v)]}e^{-i\omega_L\tau_d}$ term represents the two-photon transition that involves one XUV photon $\omega_v+\omega_L$ minus one NIR photon. The final state is at ω_v, which increases the signal at ω_v. The other two terms can be explained in the same manner. The $U(\omega_v)U(\omega_v-\omega_L)e^{i[\phi(\omega_v)-\phi(\omega_v-\omega_L)]}e^{-i\omega_L\tau_d}$ term is from the two-photon transition that involves one XUV photon ω_v minus one NIR photon. The final state is at $\omega_v-\omega_L$. This transition reduces the signal at ω_v. The $U(\omega_v)U(\omega_v-\omega_L)e^{i[\phi(\omega_v-\omega_L)-\phi(\omega_v)]}e^{i\omega_L\tau_d}$ term represents the two-photon transition that involves one XUV photon $\omega_v-\omega_L$ plus one NIR photon. The final state is at ω_v, which increases the signal at ω_v. This equation shows that the signal at momentum v is the result of interference between the two-photon (XUV + NIR) transition pathways to the final state with momentum v, as shown in Fig. 1.

Equation (9) can be simplied to:

$$\begin{aligned} I_{\omega_L}(v,\tau_d) = \frac{vE_0}{\omega_L}U(\omega_v)\{&U(\omega_v+\omega_L)\sin[\omega_L\tau_d+\phi(\omega_v)-\phi(\omega_v+\omega_L)] \\ &-U(\omega_v-\omega_L)\sin[\omega_L\tau_d+\phi(\omega_v-\omega_L)-\phi(\omega_v)]\}, \end{aligned} \quad (10)$$

#126449 - $15.00 USD Received 2 Apr 2010; revised 24 May 2010; accepted 24 May 2010; published 2 Jun 2010
(C) 2010 OSA

which oscillates with ω_L, encoding the spectral phase difference between those frequency components coupled by one NIR photon. The ω_L component can be rewritten as:

$$I_{\omega_L}(v,\tau_d) = U^2(\omega_v)\frac{vE_0}{\omega_L}\gamma(v)\sin(\omega_L\tau_d + \alpha), \tag{11}$$

where

$$\gamma(v) = \frac{I(\omega_v+\omega_L)}{I(\omega_v)} + \frac{I(\omega_v-\omega_L)}{I(\omega_v)} - 2\frac{\sqrt{I(\omega_v+\omega_L)I(\omega_v-\omega_L)}}{I(\omega_v)}\cos[\phi(\omega_v-\omega_L)-\phi(\omega_v+\omega_L)] \tag{12}$$

is proportional to the modulation depth of the oscillation, $\frac{vE_0}{\omega_L}\gamma(v)$, and

$$\tan[\alpha(v)] = \frac{\sqrt{I(\omega_v+\omega_L)}\sin[\phi(\omega_v)-\phi(\omega_v+\omega_L)] - \sqrt{I(\omega_v+\omega_L)}\sin[\phi(\omega_v-\omega_L)-\phi(\omega_v)]}{\sqrt{I(\omega_v+\omega_L)}\cos[\phi(\omega_v)-\phi(\omega_v+\omega_L)] - \sqrt{I(\omega_v+\omega_L)}\cos[\phi(\omega_v-\omega_L)-\phi(\omega_v)]} \tag{13}$$

is the tangent of the phase angle $\alpha(v)$ of the oscillation.

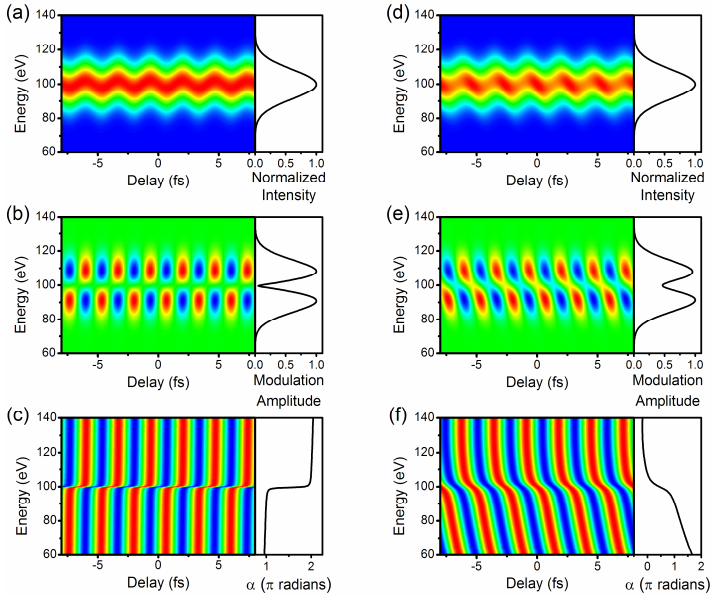

Fig. 2. Extraction of the modulation amplitude $U^2(\omega_v)(vE_0/\omega_L)\gamma(v)$ and the phase angle $\alpha(v)$ from the spectrogram for a nearly transform-limited 95 as pulse (a-c) and a strongly chirped 300 as attosecond pulse (d-f). (a, d) (left) Laser-assisted photoemission spectrogram and (right) attosecond pulse power spectrum. (b, e) (left) Filtered ω_L oscillation and (right) extracted modulation amplitude. (c, f) (left) Filtered ω_L oscillation, normalized to the peak signal at each electron energy and (right) extracted $\alpha(v)$.

As an example, the retrieval of the modulation amplitude and the phase angle $\alpha(v)$ from the filtered spectrogram $I_{\omega_L}(v,\tau_d)$ is demonstrated for two simulated spectrograms in Fig. 2. The power spectra of the pulses are identical but the spectral phases are different. In both cases, the Gaussian attosecond pulse spectrum supported 90 *as* pulses, and the dressing laser

#126449 - $15.00 USD Received 2 Apr 2010; revised 24 May 2010; accepted 24 May 2010; published 2 Jun 2010
(C) 2010 OSA

was chosen to be 20 *fs* in duration centered at 800 nm and with a peak intensity of 10^{11} W/cm^2. Clearly, the spectral phase affects both $\gamma(v)$ and $\alpha(v)$.

The spectral phase difference $\phi(\omega_v - \omega_L) - \phi(\omega_v + \omega_L)$ can be directly obtained from the modulation amplitude parameter $\gamma(v)$ by solving Eq. (12). Such a retrieval requires an accurate measurement of the dressing laser intensity to know $\gamma(v)$. Alternatively, $\phi(\omega_v) - \phi(\omega_v + \omega_L)$ and $\phi(\omega_v - \omega_L) - \phi(\omega_v)$ can be extracted from the phase angle $\alpha(v)$ by solving coupled equations Eq. (13) for each energy ω_v, taking advantage of the recurrence nature of the equations. One does not need to know the dressing laser intensity to obtain the phase angle $\alpha(v)$, which is the reason that we use $\alpha(v)$ for the phase retrieval in this work.

2.2 Minimization

When the signal-to-noise ratio is low, as is often the case in attosecond streaking experiments, the equations Eq. (13) may not have an analytical solution. The most straightforward way to extract the phase $\phi(\omega_v)$ is by minimizing the least square error function between the measured and guessed phase angles:

$$R[\phi(\omega_v)] = \left(\sum_{\omega_v} I(\omega_v) \left[\alpha(v) - \alpha'(v) \right]^2 \right)^{1/2}, \tag{14}$$

where

$$\alpha'(v) = \tan^{-1}\left[\frac{\sqrt{I(\omega_v + \omega_L)} \sin[\phi(\omega_v) - \phi(\omega_v + \omega_L)] - \sqrt{I(\omega_v + \omega_L)} \sin[\phi(\omega_v - \omega_L) - \phi(\omega_v)]}{\sqrt{I(\omega_v + \omega_L)} \cos[\phi(\omega_v) - \phi(\omega_v + \omega_L)] - \sqrt{I(\omega_v + \omega_L)} \cos[\phi(\omega_v - \omega_L) - \phi(\omega_v)]} \right] \tag{15}$$

is the phase angle calculated from the guessed values of the spectral phase. Various analytical forms of the spectral phase can be assumed. Furthermore, minimization algorithms which do not require an analytical form of the phase can also be developed.

We use an evolutionary algorithm [15] to minimize the error function $R[\phi(\omega_v)]$. For this, the spectral phase is represented as an array (chromosome) of real numbers (genes) between 0 and 2π corresponding to the phase at each energy ω_v and the algorithm is initialized with a population of randomly generated phase patterns. In this way, no assumptions are made about the phase. Reproduction is carried out using roulette wheel selection; in addition, cloning, mutation, and crossover operations are used in order to improve the speed of convergence. Furthermore, randomly generated phase patterns are added to the population periodically to increase genetic diversity and to prevent stagnation. The algorithm has been found to be quite robust, converging unequivocally to the global minimum in all tested cases.

3. Results and discussion

3.1 Experimental data

We first demonstrate the PROOF technique on a narrow bandwidth attosecond pulse generated with Generalized Double Optical Gating (GDOG) [10], as shown in Fig. 3. For such a spectrum, FROG-CRAB also works well and can serve as a benchmark. The details of the experiment are published elsewhere [14]. The dressing laser pulse was 25 fs in duration centered at 790 nm and was estimated to have an intensity of ~10^{12} W/cm^2 at the detection gas

#126449 - $15.00 USD Received 2 Apr 2010; revised 24 May 2010; accepted 24 May 2010; published 2 Jun 2010
(C) 2010 OSA

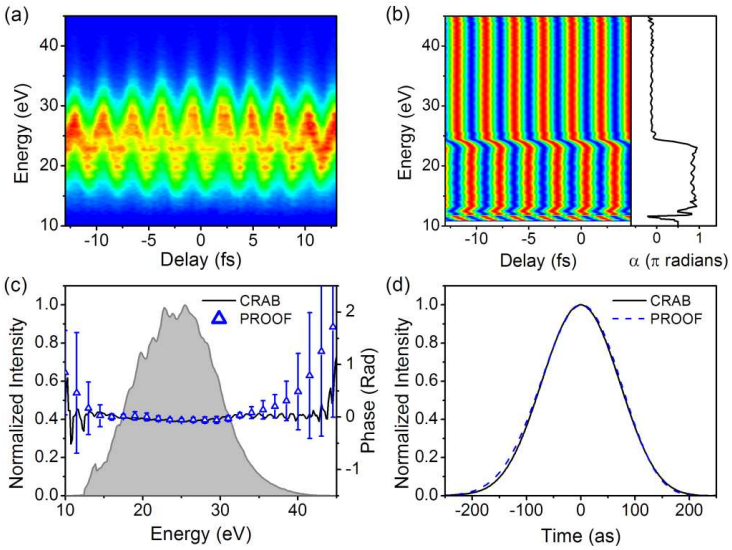

Fig. 3. Retrieval of a narrow-bandwidth attosecond pulse with PROOF. (a) Experimentally-obtained laser-assisted photoemission spectrogram. (b) (left) Filtered ω_L oscillation from the trace in (a), normalized to the peak signal at each electron energy and (right) extracted phase angle $\alpha(v)$. (c) Photoelectron spectrum (shaded) and retrieved phase from PROOF (blue triangles) and FROG-CRAB (black line). Determination of the error bars is discussed in section 3.3 (d) Retrieved pulses from PROOF (blue dash, 170 as pulse duration) and FROG-CRAB (black solid, 167 as pulse duration).

target, which is sufficient for an accurate FROG-CRAB retrieval for this spectrum [10]. The FROG-CRAB retrievals were performed with the Principal Component Generalized Projections Algorithm (PCGPA) [8,12,16]. The algorithm was run for 1000 iterations, at which point convergence had been established. Figure 3(a) shows the experimentally-obtained electron spectrogram. After spectral filtering, the ω_L contribution is shown in Fig. 3(b), which is normalized to the peak signal at each electron energy to see the phase angle $\alpha(v)$ clearly. The spectral phase is extracted from the one-dimensional phase angle array $\alpha(v)$, whereas FROG-CRAB retrieves the attosecond pulse by fitting the two-dimensional spectrogram. Finally, the retrieved XUV spectral phase and pulse are compared with those retrieved from FROG-CRAB in Figs. 2(c) and (d). Clearly, the PROOF result agrees very well with the FROG-CRAB result in this case.

3.2 Simulated data

The ability of the PROOF technique to retrieve broadband, very short attosecond pulses is demonstrated with simulated data, as experimental data is not available. Figure 4(a) shows the electron spectrogram from a complicated spectrum extending from 0 to 200 eV which supports transform-limited pulses 25 *as* in duration, with a dressing laser pulse 20 fs in duration and with peak intensity of 10^{11} W/cm^2. Spectral phase was added to give an asymmetric pulse with a pulse duration of ~73 *as*. Figures 4(c) and (d) compare the actual spectral phase and temporal profile of the pulse with those retrieved from PROOF and FROG-CRAB. Clearly, PROOF is able to fully reproduce the spectral phase and pulse profile, whereas the FROG-CRAB technique retrieves a nearly flat phase. Here, the bandwidth of the

#126449 - $15.00 USD Received 2 Apr 2010; revised 24 May 2010; accepted 24 May 2010; published 2 Jun 2010
(C) 2010 OSA

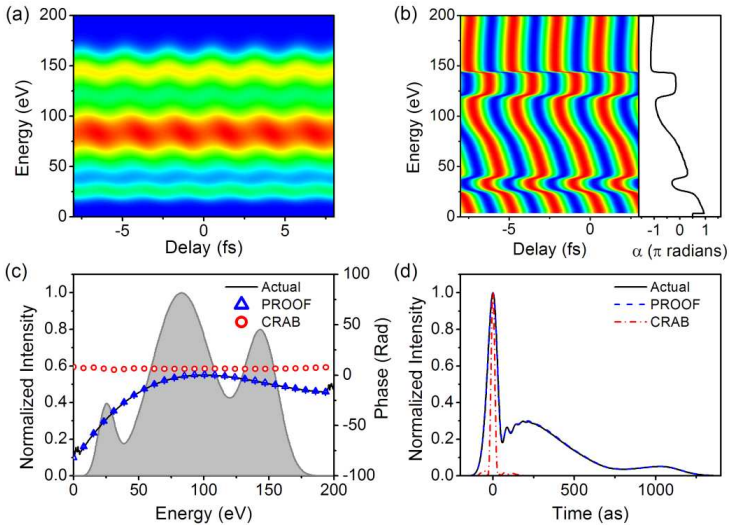

Fig. 4. Retrieval of a broad-bandwidth chirped attosecond pulse with PROOF. (a) Simulated laser-assisted photoemission spectrogram. (b) (left) Filtered ω_L oscillation from the trace in (a), normalized to the peak signal at each electron energy and (right) extracted phase angle $\alpha(v)$. (c) Photoelectron spectrum (shaded) and retrieved phase from PROOF (blue triangles) and FROG-CRAB (red circles), compared with the actual phase (black line). (d) Retrieved pulses from PROOF (blue dash, 73 as pulse duration) and FROG-CRAB (red dash-dot, 26 as pulse duration), compared with the actual pulse (black solid, 73 as pulse duration).

spectrum is larger than the central electron energy; thus the central momentum approximation for FROG-CRAB is not valid.

PROOF is compared with FROG-CRAB for a nearly transform-limited pulse with the same broad spectrum in Fig. 5. In this case, the spectral phase was chosen to vary only slightly over the spectrum, to create an asymmetric pulse with a duration of ~31 *as*. As is shown in Fig. 5(c) the phase was retrieved quite well with PROOF, whereas FROG-CRAB again underestimated the chirp. Although the two methods retrieved similar pulse durations due to the nearly-transform limited nature of both retrievals, differences are apparent in the pulse shape, shown in Fig. 5(d). Whereas PROOF retrieved the asymmetric pulse profile quite accurately, FROG-CRAB could not.

3.3 Error analysis

Because the PROOF retrieval uses only those energy components of the spectrogram that are separated by one photon energy, whereas the photoelectron spectrometer typically has much higher resolution, multiple PROOF retrievals can be performed on the same spectrogram without duplicating data. This allows for determination of error bars on the spectral phase retrieved with PROOF. In Figs. 3, 4, and 5, the PROOF retrieved phase plotted is the average of the phases obtained from retrievals using different energy pixels, weighted by the minimized error function $R[\phi(\omega_v)]$ obtained. The error bars are the weighted standard deviations of the different retrievals. This provides an additional check of the retrieval quality: if significant noise is present in the data (is is the case on the wings of the spectrum in Fig. 3, where the count rate is lower), retrievals using different energy pixels will not give the same

#126449 - $15.00 USD Received 2 Apr 2010; revised 24 May 2010; accepted 24 May 2010; published 2 Jun 2010
(C) 2010 OSA

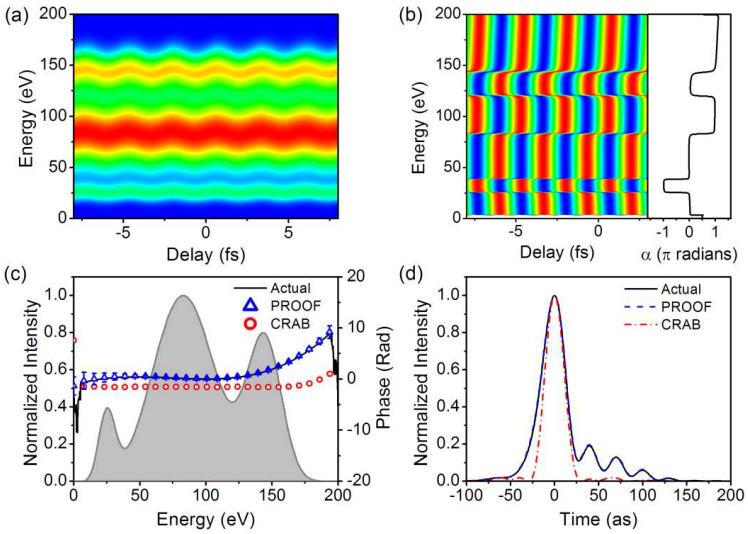

Fig. 5. Retrieval of a broad-bandwidth nearly transform-limited attosecond pulse with PROOF. (a) Simulated laser-assisted photoemission spectrogram. (b) (left) Filtered ω_L *oscillation from the trace in (a), normalized to the peak signal at each electron energy and (right) extracted phase angle* $\alpha(v)$. (c) Photoelectron spectrum (shaded) and retrieved phase from PROOF (blue triangles) and FROG-CRAB (red circles), compared with the actual phase (black line). (d) Retrieved pulses from PROOF (blue dash, 31 as pulse duration) and FROG-CRAB (red dash-dot, 25 as pulse duration), compared with the actual pulse (black solid, 31 as pulse duration).

phase pattern, and the error bars will grow to be comparable to 2π, indicating that the phase is unknown.

3.4 Dressing laser intensity

The derivation of PROOF requires that the dressing laser intensity is small and can be treated perturbatively. Under this approximation, only two-photon transition pathways can interfere, making the spectral phase encoding quite clear. However, when higher dressing laser intensities are used, and the approximation in Eq. (6) is not strictly valid (as is likely the case in Figs. 3, 4, and 5), PROOF is still able to retrieve the pulse quite well. This is shown in more detail in Fig. 6 for which spectrograms were simulated using the attosecond pulse used in Fig. 4 and dressing laser intensities ranging from 10^{10} to 10^{13} W/cm^2 and pulse retrievals were performed using PROOF and FROG-CRAB. The ability of PROOF to retrieve the pulse duration and temporal profile quite well up to more than 10^{12} W/cm^2 dressing laser intensity is likely due to the fact that the single NIR photon energy component of the spectrogram is chosen, thus eliminating the effects of many NIR photon transition pathways. The fact that FROG-CRAB is unable to accurately determine the pulse duration and profile, even when the streaking laser intensity is quite high, is very likely due to the breakdown of the central momentum approximation.

4. Conclusions

In the past, two-photon transition interference has been used to characterize the average duration of pulses in an attosecond pulse train [17]. Here we show that the ω_L component of the electron spectrogram that contains the information of the transition interference between

#126449 - $15.00 USD Received 2 Apr 2010; revised 24 May 2010; accepted 24 May 2010; published 2 Jun 2010
(C) 2010 OSA

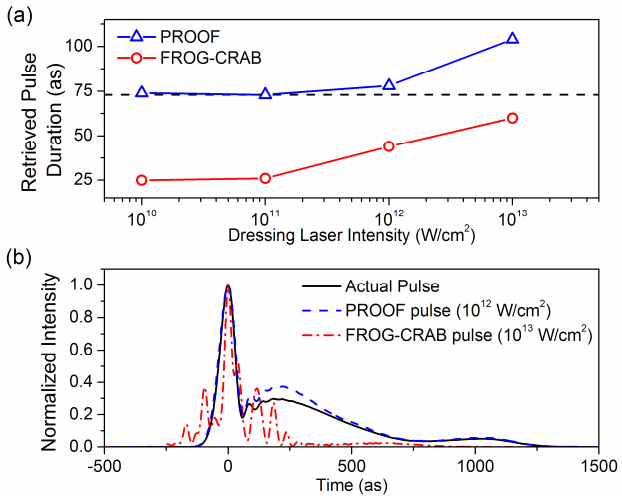

Fig. 6. Dressing laser intensity dependence of PROOF. (a) Retrieved pulse duration from PROOF and FROG-CRAB. Clearly, PROOF is able to retrieve the pulse duration accurately with dressing laser intensities from 10^{10} to 10^{12} W/cm^2, whereas FROG-CRAB fails due to the central momentum approximation. (b) Retrieved temporal profiles from PROOF with a dressing laser intensity of 10^{12} W/cm^2 and FROG-CRAB with a dressing laser intensity of 10^{13} W/cm^2. PROOF is able to retrieve the pulse quite well despite the high dressing laser intensity, whereas FROG-CRAB never retrieves the pulse shape correctly.

two-photon pathways in laser-dressed photoemission also offers a direct way to measure the relative phase of interfering states in continous XUV spectrum. We have demonstrated that the PROOF technique based on such interference can be used to characterize isolated attosecond pulses. PROOF has many advantages over other techniques, in that it is not limited to narrow bandwidth pulses and it can be performed with low dressing laser intensities. It can therefore be used to characterize the phase of recently generated gated high harmonic spectra supporting atomic unit pulse durations, or even zeptosecond pulses.

Acknowledgments

This work is supported by the U.S. Army Research Office (USARO) under grant number W911NF-07-1-0475 and by the Chemical Sciences, Geosciences, and Biosciences Division, U.S. Department of Energy (DOE).

#126449 - $15.00 USD Received 2 Apr 2010; revised 24 May 2010; accepted 24 May 2010; published 2 Jun 2010
(C) 2010 OSA